

Gene Expression Profiling in Autoimmune Noninfectious Uveitis Disease¹

Zhuqing Li,* Baoying Liu,* Arvydas Maminishkis,[†] Sankaranarayanan P. Mahesh,* Steven Yeh,* Julie Lew,* Wee Kiak Lim,*[‡] H. Nida Sen,* Grace Clarke,* Ronald Buggage,* Sheldon S. Miller,[†] and Robert B. Nussenblatt*²

Noninfectious uveitis is a predominantly T cell-mediated autoimmune, intraocular inflammatory disease. To characterize the gene expression profile from patients with noninfectious uveitis, PBMCs were isolated from 50 patients with clinically characterized noninfectious uveitis syndrome. A pathway-specific cDNA microarray was used for gene expression profiling and real-time PCR array for further confirmation. Sixty-seven inflammation- and autoimmune-associated genes were found differentially expressed in uveitis patients, with 28 of those genes being validated by real-time PCR. Several genes previously unknown for autoimmune uveitis, including *IL-22*, *IL-19*, *IL-20*, and *IL-25/IL-17E*, were found to be highly expressed among uveitis patients compared with the normal subjects with *IL-22* expression highly variable among the patients. Furthermore, we show that *IL-22* can affect primary human retinal pigment epithelial cells by decreasing total tissue resistance and inducing apoptosis possibly by decreasing phospho-Bad level. In addition, the microarray data identified a possible uveitis-associated gene expression pattern, showed distinct gene expression profiles in patients during periods of clinical activity and quiescence, and demonstrated similar expression patterns in related patients with similar clinical phenotypes. Our data provide the first evidence that a subset of *IL-10* family genes are implicated in noninfectious uveitis and that *IL-22* can affect human retinal pigment epithelial cells. The results may facilitate further understanding of the molecular mechanisms of autoimmune uveitis and other autoimmune originated inflammatory diseases. *The Journal of Immunology*, 2008, 181: 5147–5157.

Intraocular inflammatory disease or uveitis is a major cause of visual handicap in the United States, causing an estimated >100,000 new cases of ocular morbidity per year and 10% of the new cases of legal blindness (1). It has been generally accepted that noninfectious uveitis is an autoimmune disorder predominantly mediated by Th cells (2, 3). Earlier studies on humans as well as in animal models demonstrated that Th1-mediated autoimmune responses play a pivotal role in this disease (4–6). Several autoantigens have been identified as potential triggers for autoimmune uveitis (7–9). However, the varied clinical appearance in humans and the varied response to immunosuppressive regimens suggest that multiple mechanisms may be involved. For example, less than one-third of uveitis patients tested will have T cell responses to arrestin or S-Ag, the most recognized autoantigen for uveitis in humans (10). In addition, susceptibility to the two most important Ags used to induce experimental animal uveitis, interphotoreceptor retinoid-binding protein and S-Ag, varies from species to species despite evolutionarily conserved structures (11), and documented T cell response from uveitis patients to interphotoreceptor retinoid-binding protein has been scarce. Recent work

has also indicated that, similar to multiple sclerosis, Th17 cells may be one of the key immune components that contribute to the molecular pathogenesis of autoimmune uveitis (12). To facilitate the understanding of the molecular mechanisms of autoimmune uveitis and other autoimmune diseases, we investigated the gene expression profile of autoimmune uveitis using cDNA microarray and real-time PCR array on 50 clinically characterized uveitis patients. Our results identified a set of *IL-10* family genes, including *IL-22*, that are highly expressed in uveitis patients when compared with that of normal subjects, but have not been previously implicated in noninfectious uveitis. An in vitro study demonstrated that *IL-22* affected human primary retinal pigment epithelial (RPE)³ cells by decreasing their total tissue resistance, a hallmark of tissue integrity of those retinal epithelial cells (13). Meantime, *IL-22* induced apoptosis of cultured human primary RPE cells which is associated with decreased phospho-Bad level. We also show that there exists a molecular pattern for gene expression among uveitis patients compared with normal controls.

Materials and Methods

Patients, normal controls, and human fetal tissue

The research performed in this study followed the tenets of the Declaration of Helsinki and the National Institutes of Health Institutional Review Board. Fifty-eight patients with well-defined clinical diagnoses of noninfectious uveitic syndrome were enrolled into the National Eye Institute (NEI) after institutional review board approval (protocol no. 02-EI-0122). Patient consent was obtained before enrollment and the ocular status of the patients after enrollment was evaluated and recorded independently by ophthalmologists in the NEI Uveitis Clinic. Samples from 20 healthy donors as normal controls were obtained from the

*Laboratory of Immunology and [†]Section on Epithelial and Retinal Physiology and Disease, National Eye Institute, National Institutes of Health, Bethesda, MD 20892; and [‡]Singapore National Eye Center, Singapore

Received for publication March 11, 2008. Accepted for publication July 25, 2008.

The costs of publication of this article were defrayed in part by the payment of page charges. This article must therefore be hereby marked *advertisement* in accordance with 18 U.S.C. Section 1734 solely to indicate this fact.

¹ This work is supported by the Intramural Research Program of the National Eye Institute.

² Address correspondence and reprint requests to Dr. Robert B. Nussenblatt, Laboratory of Immunology, National Eye Institute, National Institutes of Health, Building 10, Room 10N112, 9000 Rockville Pike, Bethesda, MD 20892. E-mail address: DrBob@nei.nih.gov

³ Abbreviations used in this paper: RPE, retinal pigment epithelial; qRT-PCR, quantitative RT-PCR; TER, total epithelial resistance; NL, normal.

Table I. Patient information^a

	Asian Pacific	African American, Not Hispanic	Hispanic	Caucasian, Not Hispanic	Others	Total
Female	1	11	2	18	0	32 (55%)
Male	2	5	1	17	1	26 (45%)
Total	3	16	3	35	1	58
Clinical Diagnosis	Enrollment					
Intermediate uveitis	13					
Behçet disease	7					
Panuveitis	6					
Sarcoidosis	5					
VKH	5					
Anterior uveitis	4					
Retinal vasculitis	3					
Scleritis	2					
Others ^b	13					

^a Mean age, 36.7 years; range, 6–78 years.
^b Includes multifocal choroiditis, serpiginous, etc.

National Institutes of Health Blood Bank (protocol no. 97-0134). Human fetal eyes of nominal gestation of 15–17 wk were obtained from Advanced Bioscience Resources.

Cell culture on Transwell filters

Primary cell cultures of human fetal RPE cells were prepared from human fetal eyes as described previously (13). Second passage cells were seeded

in Transwells (0.4-μm pore polyester membranes; Corning Costar). Media were changed every 3 days and the cultures were maintained for at least 3 wk before experiments.

cDNA microarray analysis

PBMCs were isolated from patients or normal donors as described previously (14). Total RNA was extracted using an RNeasy kit (Qiagen). RNA

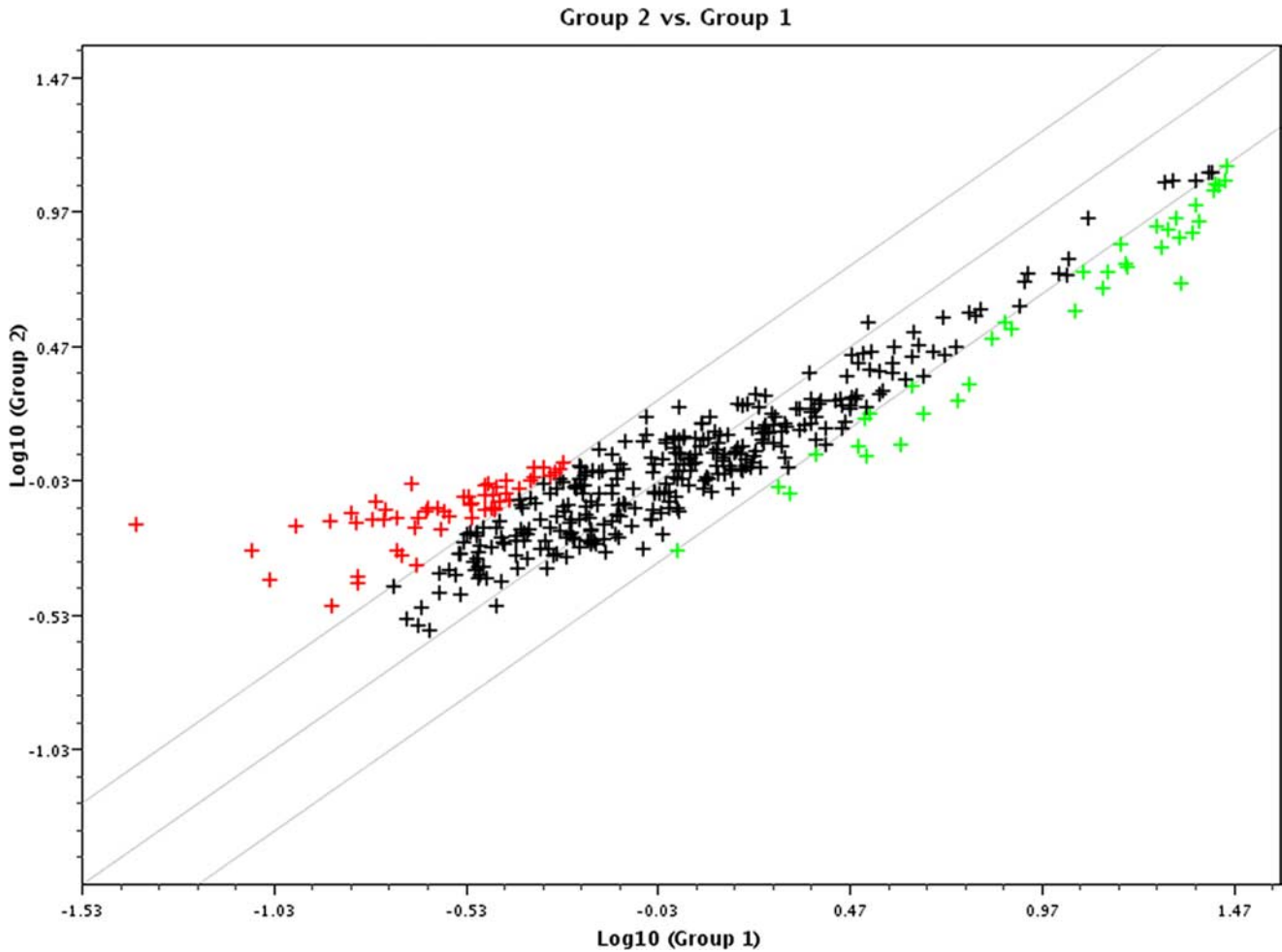


FIGURE 1. Scatter plot analysis of gene expression profiling on uveitis patients demonstrates differential gene expression. cDNA microarray analysis on 50 RNA samples from uveitis patients and 1 pooled sample from controls was performed. After normalization on housekeeping genes, e.g., *GAPDH* and β_2 -microglobulin, the final scores of each of the genes of all arrays were compared with those from the control array. The scatter plot was acquired as described in *Materials and Methods*. The y-axis represents log scores from uveitis patients (group 2) and the x-axis represents log scores from normal controls (group 1). Each symbol represents one gene with red ones representing 2-fold higher expressed in uveitis patients (group 2), green ones represent 2-fold lower expressed in uveitis patients, and the black ones represent within 2-fold cutoff threshold.

Table II. *Gene list of differentially expressed genes in uveitis patients*

Position	UniGene	Reference Sequence No.	Symbol	Description	Fold Changes
48	Hs.10458	NM_004590	CCL16	Chemokine (C-C motif) ligand 16	16.6
171	Hs.168132	NM_172175	IL-15	IL-15	7.6
62	Hs.251526	NM_006273	CCL7	Chemokine (C-C motif) ligand 7	5.9
112	Hs.201300	NM_006639	CYSLTR1	Cysteinyl leukotriene receptor 1	5.6
174	Hs.41724	NM_002190	IL-17	IL-17 (CTL-associated serine esterase 8)	5.0
192	Hs.73917	NM_000589	IL-4	IL-4	5.0
63	Hs.271387	NM_005623	CCLB	Chemokine (C-C motif) ligand 8	4.6
172	Hs.524117	NM_002189	IL-15RA	IL-15R α	4.4
64	Hs.301921	NM_001295	CCR1	Chemokine (C-C motif) receptor 1	4.4
80	Hs.1634	NM_001789	CDC25A	Cell division cycle 25A	4.1
222	Hs.498997	NM_014387	LAT	Linker for activation of T cells	3.8
252	Hs.153629	NM_005919	MEF2B	MADS box transcription enhancer factor 2, polypeptide B (myocyte enhancer factor 2B)	3.4
96	Hs.2233	NM_000759	CSF3	Colony-stimulating factor 3 (granulocyte)	3.4
239	Hs.531754	NM_145185	MAP2K7	MAPK kinase 7	3.3
185	Hs.272373	NM_018724	IL-20	IL-20	3.0
368	Hs.75516	NM_003331	TYK2	Tyrosine kinase 2	2.9
237	Hs.134859	NM_005360	MAF	V-maf musculoaponeurotic fibrosarcoma oncogene homolog (avian)	2.8
89	Hs. 172928	NM_000088	COL1A1	Collagen, type I, α 1	2.8
157	Hs. 43505	NM_003639	IKBKKG	Inhibitor of κ light polypeptide gene enhancer in B cells, kinase γ	2.7
254	Hs.497723	AF067420	MGC27165	Hypothetical protein MGC27165	2.7
158	Hs.193717	NM_000572	IL-10	IL-10	2.7
255	Hs.126714	NM_000246	CIITA	Class II, MHC, transactivator	2.7
127	Hs.513470	NM_032815	NFATC2IP	NF-AT, cytoplasmic, calcineurin-dependent 2 interacting protein	2.7
253	Hs.314327	NM_005920	MEF2D	MADS box transcription enhancer factor 2, polypeptide D (myocyte enhancer factor 2D)	2.6
139	Hs.466828	NM_019884	GSK3A	Glycogen synthase kinase 3 α	2.6
335	Hs.517148	NM_016397	TH1L	TH1-like (<i>Drosophila</i>)	2.5
191	Hs.694	NM_000588	IL-3	IL-3 (colony-stimulating factor, multiple)	2.5
160	Hs.418291	NM_000628	IL-10RB	IL-10R β	2.5
236	Hs.123119	NM_005905	SMAD9	SMAD, mothers against DPP homolog 9 (<i>Drosophila</i>)	2.5
187	Hs.465645	NM_019107	C19orf10	Chromosome 19 open reading frame 10	2.4
169	Hs.336046	NM_000640	IL13RA2	IL-13R α 2	2.4
328	Hs.133379	NM_003238	TGFB2	TGF- β 2	2.4
223	Hs.194236	NM_000230	LEP	Leptin (obesity homolog, mouse)	2.4
141	Hs.155111	NM_032782	HAVCR2	Hepatitis A virus cellular receptor 2	2.4
313	Hs.468426	NM_144949	SOCS5	Suppressor of cytokine signaling 5	2.4
207	Hs.436061	NM_002198	IRF1	IFN regulatory factor 1	2.3
170	Hs.17987	L15344	TXLNA	Taxilin α	2.3
7	Hs.465709	NM_000635	RFX2	Regulatory factor X, 2 (influences HLA class II expression)	2.3
121	Hs.86131	NM_003824	FADD	Fas (TNFRSF6)-associated via death domain	2.3
334	Hs.373550	NM_003244	TGIF	TGFB-induced factor (TALE family homeobox)	2.3
67	Hs.184926	NM_005508	CCR4	Chemokine (C-C motif) receptor 4	2.3
6	Hs.73677	NM_002918	RFX1	Regulatory factor X, 1 (influences HLA class II expression)	2.3
256	Hs.407995	NM_002415	MIF	Macrophage migration inhibitory factor (glycosylation-inhibiting factor)	2.2
159	Hs.504035	NM_001558	IL-10RA	IL-10R α	2.2
109	Hs.89714	NM_002994	CXCL5	Chemokine (C-X-C motif) ligand 5	2.2
224	Hs.36	NM_000595	LTA	Lymphotoxin α (TNF superfamily, member 1)	2.2
153	Hs.450230	NM_000598	IGFBP3	Insulin-like growth factor-binding protein 3	2.2
272	Hs.9731	NM_002503	NFKBIB	Nuclear factor of κ light polypeptide gene enhancer in B cells inhibitor, β	2.1
106	Hs.100431	NM_006419	CXCL13	Chemokine (C-X-C motif) ligand 13 (B cell chemoattractant)	2.1
156	Hs.321045	NM_014002	IKBKE	Inhibitor of κ light polypeptide gene enhancer in B cells, kinase ϵ	2.1
251	Hs.268675	NM_005587	MEF2A	MADS box transcription enhancer factor 2, polypeptide A (myocyte enhancer factor 2A)	2.1
221	Hs.409523	NM_002286	LAG3	Lymphocyte-activation gene 3	2.1
143	Hs.515126	NM_000201	ICAM1	ICAM 1 (CD54), human rhinovirus receptor	2.1
24	Hs.437877	NM_020547	AMHR2	Anti-Mullerian hormone receptor, type II	2.1
47	Hs.272493	NM_004167	CCL15	Chemokine (C-C motif) ligand 15	2.0
286	Hs.1976	NM_002608	PDGFB	Platelet-derived growth factor β polypeptide (simian sarcoma viral (v-sis) oncogene homolog	2.0
235	Hs.465087	NM_005904	SMAD7	SMAD, mothers against DPP homolog 7 (<i>Drosophila</i>)	0.5

(Table continues)

Table II. (Continued)

Position	UniGene	Reference Sequence No.	Symbol	Description	Fold Changes
75	Hs.2259	NM_000073	CD3G	CD3G antigen, gamma polypeptide (TiT3 complex)	0.5
195	Hs.68876	NM_000564	IL-5RA	IL-5R α	0.5
263	Hs.529244	NM_003581	NCK2	NCK adaptor protein 2	0.5
325	Hs.170009	NM_003236	TGFA	TGF α	0.4
200	Hs.624	NM_000584	IL-8	IL-8	0.4
274	Hs.2764	NM_005007	NFKBIL1	Nuclear factor of κ light polypeptide gene enhancer in B cells inhibitor-like 1	0.4
347	Hs.211600	NM_006290	TNFAIP3	TNF α -induced protein 3	0.4
242	Hs.145605	NM_006609	MAP3K2	MAPK kinase kinase 2	0.4
181	Hs.126256	NM_000576	IL-1B	IL-1 β	0.4
215	Hs.525704	NM_002228	JUN	V-jun sarcoma virus 17 oncogene homolog (avian)	0.3

isolated from 20 healthy donors were pooled and served as normal controls. Biotinylated probes were generated from 5 μ g of total RNA from each RNA sample by incorporating biotinylated dUTP into synthesized cDNAs using a T7 polymerase linear amplification strategy. Probes were hybridized to a pathway-specific cDNA microarray chip (Inflammatory and Autoimmune GEArray; SuperArray). Signals for specific binding were recorded by a charge-coupled device camera. A total of 51 microarray analyses were performed independently for all patient samples and one pooled normal sample. Gene expression profiling was analyzed using GEArray Suite software (SuperArray). Briefly, acquired digital images were aligned, computed for density, normalized based on negative controls, and transformed into scores for gene expression based on an established algorithm (SuperArray). All scores for each gene in one array were then normalized on housekeeping genes, e.g., *GAPDH* and β_2 -microglobulin. The final scores of each of the genes of all arrays were then compared with those from a control array to obtain a ratio value. A 2-fold cutoff threshold was used to define whether one gene is up-regulated or down-regulated, e.g., the expression of one gene from array X is ≥ 2 -fold of that from the control array is considered an up-regulated gene, while ≤ 0.5 -fold of the score from the same gene compared with the control array is considered a down-regulated gene. The scatter plot and clustergram were acquired using the same software according to the manufacturer's instructions.

Real-time PCR analysis

Real-time PCR array analysis was performed to confirm microarray results. A total of 60 autoimmune and inflammatory disease-related genes were examined for confirmation purposes by real-time PCR using a commercially available real-time PCR RT² Profiler Kit (SuperArray). To correlate the clinical status of the uveitis condition to the gene expression profile, only samples from patients with clinically active disease were used for real-time PCR analysis. Active uveitis was defined as evidence of cells and flare in the anterior chamber of the eye or cells and haze in the posterior chamber of the eye. A total of 42 RNA samples from clinically active uveitis patients was pooled to compare with the pooled normal control sample. Two independent PCR array analyses were performed according to the manufacturer's instructions. Briefly, 1 μ g of each of the RNA samples from either uveitis patients or normal controls were reverse-transcribed into cDNAs using a first-strand cDNA RT kit (SuperArray). Real-time PCR was performed using a 96-well format PCR array and an Applied Biosystems 7500 real-time PCR unit. Primers for all genes for real-time PCR confirmation of the microarray analysis had been pretested and confirmed by the manufacturer. Assay controls include positive and negative controls as well as three sets of housekeeping gene controls for normalization purposes. Analysis of real-time PCR results was performed according to the manufacturer's instructions (SuperArray). Data analysis is based on the $\Delta\Delta C_t$ method with normalization of the raw data to housekeeping genes as described in the manufacturer's manual. The detailed instruction for calculation and normalization can be found in the following web site: www.superarray.com. A 2-fold cutoff threshold was used to define whether one gene is up-regulated or down-regulated. To further confirm *IL-22* expression results based on microarray and real-time PCR array data, a SYBR Green-based quantitative RT-PCR (qRT-PCR) was used to analyze *IL-22* expression between normal and uveitis patients. Briefly, RNA samples from 6 normal donors and 40 uveitis patients were tested for *IL-22* gene expression using the qRT-PCR MasterMix from SuperArray following their Endpoint RT-PCR Manual. Human *GAPDH* gene expression from the same RNA samples was also tested for normalization and quantification purposes. The results were expressed as the fold expression of *IL-22* normalized on that of *GAPDH*. The *IL-22* expression was considered not

detectable if the ratio of *IL-22* against *GAPDH* is smaller than 0.001. qRT-PCR primers for *IL-22* and *GAPDH* were both from SuperArray and have been verified by the provider.

Western blot analysis

frPE cells were cultured in the presence or absence of 50 ng/ml recombinant human *IL-22* (PeproTech) for 48 h. Cells were then lysed in 100 μ l of lysis buffer [50 mM Tris-Cl, 1% Triton X-100, 100 mM NaCl, 2 mM EDTA, 50 mM NaF, 50 mM glycerol phosphate, 1 mM NaVO₄, and 1 \times protease inhibitor mixture (Roche Molecular Biochemicals)]. Complete cell lysis was achieved by immediately vortexing and then boiling in an equal amount of 2 \times SDS protein-loading buffer at 95°C for 5 min. Cell debris was removed by centrifugation at 12,000 rpm for 3 min. Twenty microliters of each sample was loaded into a 12% SDS-polyacrylamide gel with a 4% stacking gel. For immunoblotting, primary Ab of anti-phospho-Bad was purchased from Cell Signaling Technology. Anti- β -actin Ab was purchased from Santa Cruz Biotechnology.

Resistance and apoptosis assay for RPE cells

The RPE monolayers on inserts with total tissue resistance (TER) above 100 Ω cm² were cultured with either RPE culturing medium alone or in the presence of 50 ng/ml human rIL-22 (PeproTech). After 72 h of stimulation with *IL-22* of RPE monolayers on inserts, TER was measured using EVOM (World Precision Instruments). Data are expressed as mean \pm SE; statistical significance (Student's *t* test, two tail) was accepted as *p* < 0.05. For apoptosis analysis, experimental cells from the same experiments as described above were stained by annexin V (BD Bioscience) after 72 h of culturing. Samples were acquired by a FACSCalibur flow cytometer and analyzed using FlowJo software (Tree Star).

Results

Differential gene expression among uveitis patients and normal subjects

A total of 58 patients were enrolled into our microarray protocol. Table I summarizes the clinical information of all patients who were enrolled. The diagnoses, gender, race, and clinical manifestations of the enrolled patients represent what is typically seen in the Uveitis Clinic of the NEI. Eight RNA samples did not qualify for the microarray analysis after the quality control test. To test the validity of our strategy to use pooled RNA samples from normal donors as the reference RNA sample to compare with individual RNA samples from uveitis patients, we ran microarray on nine RNA samples, eight individual RNA samples from normal donors vs the pooled RNA sample from the same donors. A side-by-side analysis showed that the data derived from the eight individual donors vs the pooled sample from normal donors are very similar. Based on statistical correlation analysis, the average *p* value of correlation of the microarray data between the pooled vs the eight individual RNA samples is 0.88 (0.86–0.91). In addition, clustergram analysis also demonstrated that there was a great similarity of gene expression patterns among the eight individual normal donors when compared with the pooled RNA sample from the same donors (data not shown). Therefore, a total of 51 RNA samples, 50

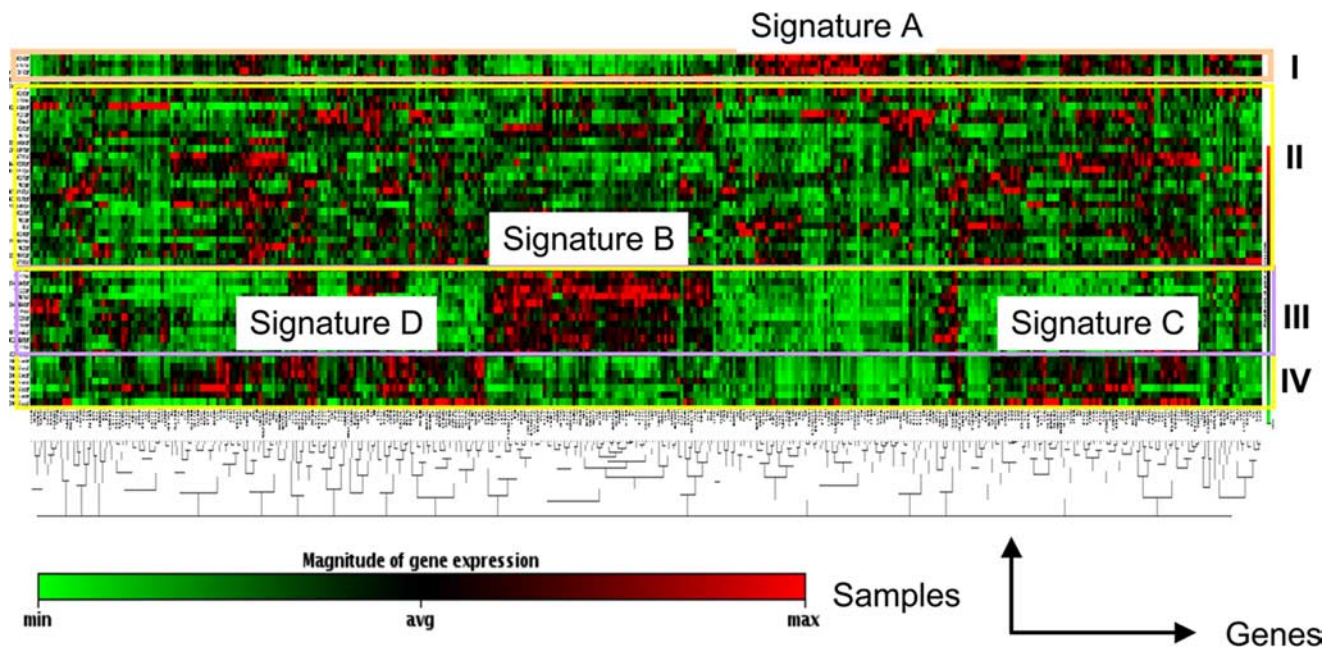


FIGURE 2. Clustergram analysis of gene expression revealed four distinct gene expression profiles. cDNA microarray was performed as described above and clustergram analysis on microarray data is described in *Materials and Methods*. The *x*-axis represents all genes listed in the cDNA microarray chip and *y*-axis depicts gene expression profiles from all samples of uveitis patients normalized on normal controls. Each colored band represents expression of a single gene from one patient when compared with that from normal donors with higher expression in red and lower expression in green. Groups I, II, III, and IV designate four subgroups of gene expression profiles. Analysis of gene expression profiling among uveitis patients revealed four sets of genes designated as molecular signatures A, B, C, and D that can be used to define the four subgroups of gene expression profiles.

from patients and 1 reference RNA pooled from 20 healthy donors, were analyzed for microarray analysis. Despite the high heterogeneity of gene expression among patients and between patients and controls, there were clear differences in gene expression patterns comparing those from patients to those from the normal pooled

control RNA. Fig. 1 is a scatter plot analysis showing genes that were differentially expressed among uveitis patients when compared with the normal donors, with red symbols representing up-regulated genes and green symbols representing down-regulated genes. When a 2-fold cutoff threshold was applied, there was a

FIGURE 3. List of the gene symbols for the four sets of molecular signatures A, B, C, and D that define subgroups of gene expression profiles. The four sets of genes were determined based on the results of clustergram analysis and expression levels of the clustered genes within each subgroup. The gene symbols were then extracted from the total gene list. The proposed functional association of genes within each set was also indicated.

A	B	C	D		
MAPK10 NCAM1 IL16 IL2RG SCYE1 MAP2K4 MAP3K1 STAT1 PAK1 NFKB2 STAT4 FCER2 CD3Z CREB1 GSK3B IKKBK COL3A1 GSK3A TXLNA TDGF1 TLR3	MAPK14 SMAD2 PTPRC TLR4 RAF1 TBX21 SELPLG NFAT5 NFATC3 CCR2 CALM2 TLR2 MAPK3 SELL CSF1 SP3 TRADD TNFRSF1A TNFRSF8 CCL2	TRAF3 TLR9 TRAF2 TRAF6 TNFRSF11A TRAF5 TGIF TH1L PDGFB SDF2 TNFRSF1B TNFRSF21 TSC22D1 TNFRSF7 TYK2 CXCL3 CD80 FKBP1B IL15 IL15RA SMAD7 FGF2 CXCL5 HAVCR2 IKBK IL2RA NFKB1 MAF MEF2D SMAD9 MEF2B	MAPK9 GATA4 ACVR2A BMPR2 RFX5 CALM1 GUSB GUSB GUSB CX3CR1 XCL2 ACVRL1 C3 AGT CABN1 CCL21 CCR7 ACVR1B BMPR1B ACVR2B BMPR1A MAP3K14 IL18R1 IL1A IL5RA ITGB7 IL5 IVL CCL17 CCL19 CEBPA CCR3 CCR4 CCL18 CCR5 CSNK2A1 EGR1 CDKN1A CSNK2B IL11 EGR3 FOSL2 GFI1 ICAM3	IL6 IL12RB1 IL1R1 IL7 IL13 IFNB1 IL12RB2 IL11RA IL18BP FOSL1 ICAM4 CTLA4 FST ICAM5 ELK3 ICOS ENG IL6R CHRD CHUK CXCL10 EP300 JAK3 SMAD3 REL JAK2 LTBR SMAD1	CCL23 BAD CALM3 SOCS2 SERPINE1 TFCP2 CXCL1 ELK1 EGR2 IL4R CDKN2B CCR10 FOS IL19 IL8RB LTBR IL9 SOCS1 TGFB1 IRAK1 PIA PIA PIA RFXDC1
Proliferative pathways	Apoptotic pathways	Cytokines/chemokines			

Table III. Differentially expressed genes in uveitis patients confirmed by real-time PCR

Up-Regulated Genes			Down-Regulated Genes		
Gene Symbol	Fold Up	NCBI Reference Sequence	Gene Symbol	Fold Down	NCBI Reference Sequence
<i>IL-22</i>	16.5	NM_020525	<i>CCL11</i>	−3.4	NM_002986
<i>GDF5</i>	7.6	NM_000557	<i>IL-8</i>	−3.7	NM_000584
<i>IL-19</i>	7.0	NM_013371	<i>CXCL14</i>	−5.2	NM_004887
<i>CX3CR1</i>	6.1	NM_001337	<i>CXCL2</i>	−5.4	NM_002089
<i>IL-20</i>	5.4	NM_018724	<i>IL-1B</i>	−6.3	NM_000576
<i>FASLG</i>	3.2	NM_000639	<i>IL-6</i>	−7.8	NM_000600
<i>CCL21</i>	3.0	NM_002989	<i>CCL18</i>	−11.9	NM_002988
<i>GDF10</i>	2.9	NM_004962	<i>CSF2</i>	−19.3	NM_000758
<i>IL-5</i>	2.8	NM_000879	<i>CCL20</i>	−21.7	NM_004591
<i>CCL19</i>	2.6	NM_006274	<i>CCL7</i>	−24.0	NM_006273
<i>CCR2</i>	2.6	NM_000648			
<i>LTB</i>	2.5	NM_002341			
<i>TNFSF10</i>	2.5	NM_003810			
<i>CXCL13</i>	2.5	NM_006419			
<i>IFNA2</i>	2.3	NM_000605			
<i>IL-4</i>	2.2	NM_000589			
<i>IL-17E</i>	2.1	NM_022789			
<i>IL-16</i>	2.1	NM_004513			

total of 67 genes (16.7%) that were differentially expressed among uveitis patients when compared with normal controls, with 56 genes up-regulated and 11 genes down-regulated among the 400 inflammatory and autoimmune disease-associated genes in this pathway-specific cDNA array chip. A complete list of differentially expressed genes (2-fold cutoff) from cDNA microarray results for uveitis is provided in Table II.

Gene expression profiling revealed four distinct subgroups of uveitis patients

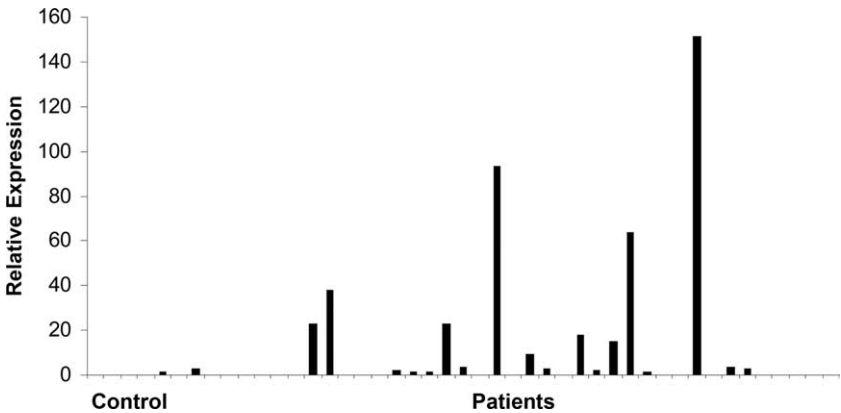
Noninfectious uveitis is considered a heterogeneous group of diseases comprised of a variety of clinical diagnoses and manifestations but all demonstrating intraocular inflammation. Based on this notion, we compared the differential gene expression patterns among uveitis patients using a density clustergram analysis with a red band representing higher and green representing lower gene expression after normalization to controls. There were clearly four distinct profiles (I, II, III, and IV) based on their unique patterns of gene expression (Fig. 2). A detailed analysis of genes in those four profiles revealed four sets of genes with higher expression that define the differential gene expression profiling. A gene list for those four sets of genes, termed as signatures A, B, C, and D, is shown in Fig. 3. It is of interest that the genes within each set appeared functionally related. For example, genes in set A were more functionally associated with cell proliferative responses, genes in set B were more associated with cell apoptosis while most cytokine/chemokines were clustered in sets C and D. One intriguing

question is whether these molecular signatures reflect distinct molecular pathogenesises for autoimmune uveitis. However, our efforts to correlate clinical uveitic diagnoses with this differential gene expression profiling were not successful (see Discussion for details).

Real-time PCR-validated gene list provides evidence of involvement of previously uncharacterized genes in autoimmune uveitis

We then used quantitative real-time PCR to validate the microarray results. As shown in Table III, real-time PCR analysis confirmed 18 up-regulated genes and 10 down-regulated genes in active uveitis patients as compared with those in normal controls (2-fold cutoff threshold). Some of the genes have been previously reported in association with autoimmune uveitis, e.g., *CX3CR1*, *CCL19*, *CCL21*, *FasL*, *IFN-α*, *IL-4*, *IL-5*, *IL-6*, and *IL-8*. However, several genes identified have not been previously associated with autoimmune uveitis including several cytokines from the *IL-10* family and one cytokine from the *IL-17* family. One set of *IL-10* family genes including *IL-19*, *IL-20*, and *IL-22*, were of particular interest. *IL-10* has been implicated to play a protective role in the mouse experimental autoimmune uveoretinitis model and is up-regulated in human uveitis patients (6, 15, 16). However, *IL-19*, *IL-20* and *IL-22* have not been implicated in human uveitis. In addition, *IL-25/IL-17E*, which belongs to the *IL-17* cytokine family, has also not been reported to be associated with autoimmune

FIGURE 4. The expression of *IL-22* in normal donors and uveitis patients. A SYBR Green-based real-time PCR analysis was performed to analyze *IL-22* mRNA levels in both normal donors and uveitis patients as described in Materials and Methods. Each bar on the x-axis represents one RNA sample from either normal donors or uveitis patients subjected to real-time PCR analysis for *IL-22* transcript. The y-axis represents relative expression of *IL-22* levels.



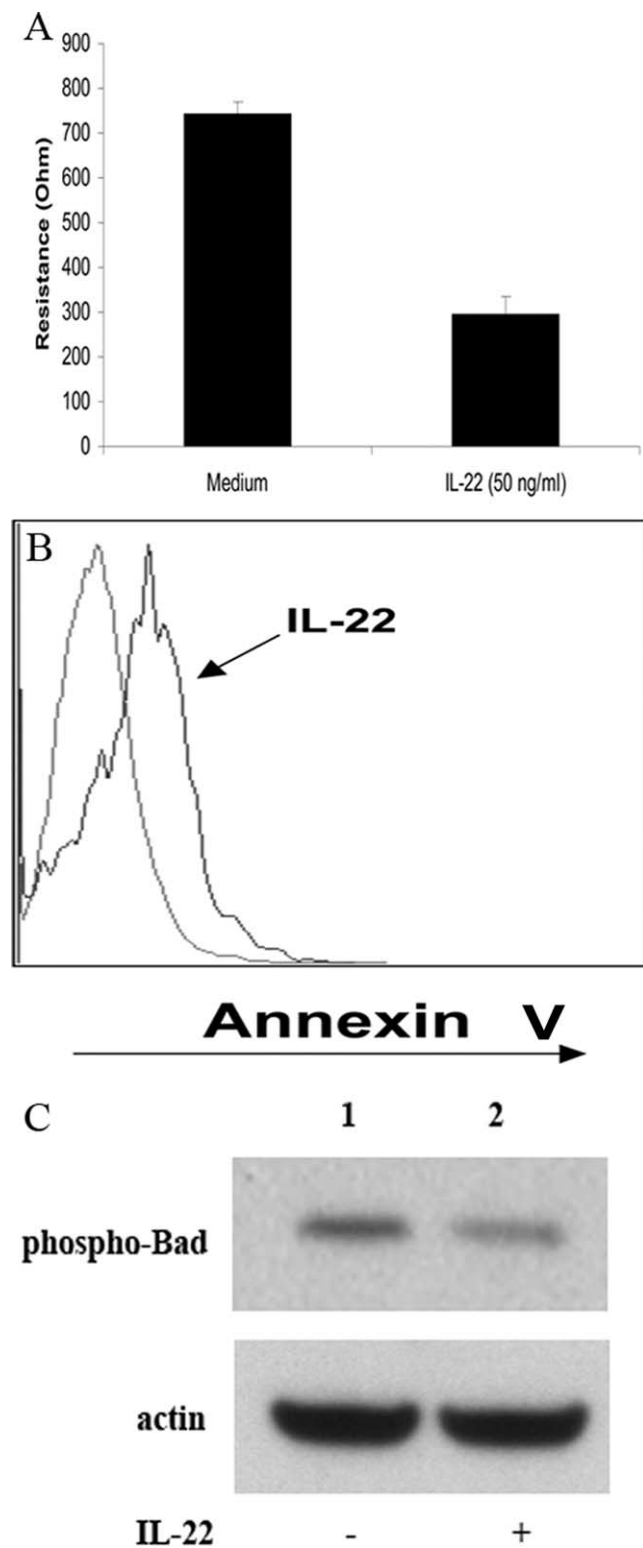


FIGURE 5. IL-22 decreased total tissue resistance and induced apoptosis of primary human RPE cells. Monolayers of RPE cells grown on inserts were treated with recombinant human IL-22 (50 ng/ml). Resistance measurements and an apoptosis assay were performed after 72 h of incubation with IL-22 as described in *Materials and Methods*. **A**, Summary bar graph of TER changes after addition of IL-22 to human fetal RPE monolayers. Compared with matched controls, TER significantly ($\sim 60\%$) decreased in IL-22-treated monolayers of RPE ($n = 3$, $p < 0.01$). **B**, A histogram comparing annexin V staining for human primary RPE cells with and without IL-22 treatment. The gray line is for the control group while the bolded dark line is for IL-22-treated RPE cells. There is a right shift of annexin V staining for IL-22-treated RPE cells when compared with the nontreated

uveitis. Genes that have not been previously reported to be associated with autoimmune uveitis are highlighted in bold and italic in Table III. To further confirm the microarray and real-time PCR array data, we tested *IL-22* gene expression in 6 normal donors and 40 uveitis patients by using a SYBR Green-based qRT-PCR strategy. As shown in Fig. 4, five of six normal donors had no detectable *IL-22* transcript except 1 donor showed a very low level of *IL-22* expression by real-time PCR. However, 25 (62.5%) of 40 uveitis patients tested positive for *IL-22* expression, with some patients demonstrating very high levels of *IL-22* expression.

IL-22 affects human primary pigment epithelial cells by decreasing their total tissue resistance and inducing apoptosis

The expression of IL-22 has been recently shown to be associated with Th17 cells (17, 18). The primary target cells for IL-22 appeared to be epithelial cells (19, 20). To further understand the possible physiological impact and molecular mechanisms of IL-22 on ocular disease, we examined the effect of IL-22 on TER and the induction of apoptosis of human RPE cells. The retinal pigment epithelium forms the outer blood-retina barrier which physically separates the subretinal space and the choroidal blood supply and actively participates in the creation of the immune-privileged retinal environment by secreting various cytokines and chemokines (unpublished data). Both TER and apoptosis assays examine the physiological integrity of the retinal pigment epithelium, which is critical to preservation of the outer blood-retina barrier. As shown in Fig. 5, after 72 h of stimulation, IL-22 significantly decreased TER by $>60\%$ as compared with matched controls ($p < 0.01$). TER decreased from 742 ± 29 to $296 \pm 37 \Omega \text{ cm}^2$ (Fig. 5A). IL-22 also induced RPE apoptosis when compared with the controls (Fig. 5B). To further understand the mechanisms of IL-22 inducing apoptosis of RPE cells, we examined several proteins that are known to be involved in the apoptosis signaling pathway, including cleaved caspase 3 and poly(ADP-ribose) polymerase and phospho-Bad. We found that IL-22 seemed primarily targeting phosphorylated-Bad. As shown in Fig. 5C, IL-22 treatment resulted in decreased phospho-Bad expression in RPE cells. However, there was no significant change in the levels of cleaved (active) caspase 3 and poly(ADP-ribose) polymerase expression, which are also known to be involved in the apoptosis pathway (data not shown). This is the first evidence that IL-22 can target the human RPE cells and potentially change their tissue integrity and preservation of the blood retinal barrier.

Gene expression profiling on patient samples at distinct clinical stages

An important characteristic of uveitis is recurrence of disease (21). However, it is not clear for clinicians if this is a new inflammatory episode or is still simply the previous episode that has lingered. To address this question, we continuously monitored one patient over a 5-mo span and collected samples during three distinct periods of disease activity, e.g., active, quiescent, and recurrent/active stages. Interestingly, there were very few changes in gene expression profiling for the samples collected at the three time points which represented three distinct clinical stages. As shown in Fig. 6, arrays 1, 2, and 3 represent gene expression patterns when the disease was

control group, indicating increased apoptosis induced by IL-22 treatment. **C**, Monolayers of RPE cells grown on inserts were treated with or without recombinant human IL-22 (50 ng/ml) for 48 h and cells were lysed and subjected to Western blot analysis for phosphorylated Bad. Although the β -actin levels were comparable comparing IL-22-treated and untreated groups, the phosphorylated Bad was decreased after IL-22 treatment.

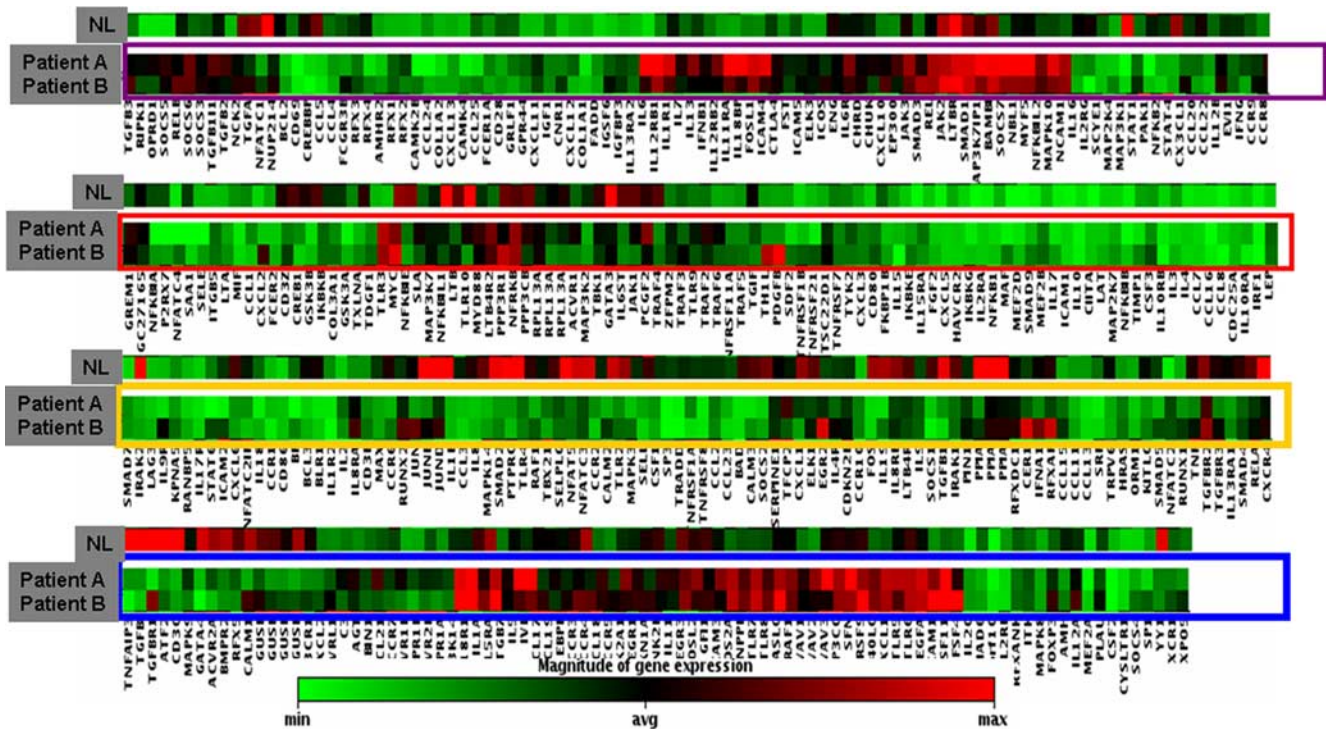


FIGURE 7. Comparison of clustergram analysis of gene expression profiling of two male siblings (designated as patient A and patient B) with the same diagnosis of intermediate uveitis with that from normal controls (designated as NL). The cDNA microarray and clustergram analysis were performed as described above and in *Materials and Methods*. The x-axis listed all of the gene symbols in the cDNA microarray chips. The gene expression profiles from the two male siblings with the same diagnosis of intermediate uveitis (designated as patient A and patient B) were aligned with the profile from normal subjects (NL). As described above, each colored band represents expression of a single gene from either patient A or patient B or from normal subjects after normalization on housekeeping genes, with higher expression in red and lower expression in green.

identified 28 genes that were either up- or down-regulated in the peripheral blood of uveitis patients with active disease when compared with normal control (Table III). The majority of those genes (19 of 28) have been previously reported to be associated with autoimmune uveitis, further validating the results of our study. However, among those up-regulated genes confirmed by real-time PCR, a set of *IL-10* family genes, including *IL-19*, *IL-20*, and *IL-22* which have not been previously associated with autoimmune uveitis, is of particular interest. *IL-10* has been implicated to play a protective role in the mouse experimental autoimmune uveoretinitis model and is up-regulated in human uveitis patients (6, 15, 16). However, *IL-19*, *IL-20*, and *IL-22* have not been implicated in human uveitis. The expression of *IL-22* has been recently associated with Th17 cells (17, 18), a newly characterized Th cell subpopulation that is believed to primarily contribute to the pathogenesis of some Th1-mediated autoimmune diseases such as multiple sclerosis (26–28). Th17 cells have also been implicated in the pathogenesis in a mouse uveitis model (12). *IL-22* has little regulatory effect on immune cells but has primarily an effect on target tissues (29). It has been suggested that *IL-22* may play an important role in autoimmune diseases such as psoriasis and ulcerative colitis (19, 20). Recently, *IL-22* has been shown to interrupt the blood-brain barrier tight junctions both in vitro and in vivo and it therefore promotes Th17 cells to transmigrate through the blood-brain barrier (30). The blood-retina barrier, similar to the blood-brain barrier, is well known to be critical for the maintenance of intraocular homeostasis. Since Th17 cells have been implicated in the pathogenesis of autoimmune uveitis (12), we tested the effect of *IL-22* on human primary RPE. The data show that *IL-22* dramatically reduces total tissue resistance of human RPE cells and that *IL-22* also induces RPE apoptosis (Fig. 5). The decrease of

TER and the induction of apoptosis of RPE cells by *IL-22* may have significant physiological and pathophysiological consequences in the eye. Epithelial electrical resistance measurement can be directly correlated to some barrier properties where in many cases TER decrease would result in an epithelial monolayer permeability increase (31–33). The reduction in TER would be consistent with the opening of a pathway that would allow biologically active molecules and immune system components to reach the site of retinal inflammatory injury in vivo (34, 35). Our data also showed that *IL-22* decreased the phospho-Bad level (Fig. 5C) and that might have contributed to the induced apoptosis of fetal RPE cells. These data have not been reported in the literature and further investigation on the effect of *IL-22* on phospho-Bad and its downstream signaling pathway will be very interesting. Overall, the data of *IL-22*'s effect on total tissue resistance as well as on inducing apoptosis suggests that *IL-22* can affect the tissue integrity of RPE cells. Because RPE cells are critical for maintaining the blood-retina barrier, we propose that *IL-22* may target human RPE cells. Similar to what has been demonstrated in multiple sclerosis that *IL-22* affects the blood-brain barrier (30), *IL-22* may disrupt the blood-retina barrier by reducing RPE total epithelial resistance (TER) and inducing RPE apoptosis. We suggest that this may be one molecular mechanism for uveitis pathogenesis. Our findings provide the first evidence that directly links *IL-22* with human intraocular inflammatory disease.

One of the other applications of gene expression profiling for clinical immunology is for molecular diagnoses such as in cancer (25, 36) or in autoimmune and inflammatory diseases (37, 38). We sought to correlate those four subgroups of gene expression profiles with clinical diagnoses and manifestations. However, we were not able to directly link the gene expression-profiling data with

clinical diagnoses. For example, patients with the diagnosis of intermediate uveitis can exhibit all four of the gene expression profiles. It is an intriguing question as to whether these molecular signatures can reflect distinctive molecular pathogenesis for autoimmune uveitis. Since all patients received at least two immunosuppressive agents for therapy, it is unlikely that immunosuppression would cause significant impact on the distinct molecular profiling results which resulted in the failure of correlation of clinical manifestation with the molecular profiling data. We propose, based on our data, that clinical manifestations may not necessarily be able to be correlated with molecular pathways of uveitic syndromes. In fact, similar observations have been made in large B cell lymphoma with no common set of genes expressed in all cases (39–41). We suggest that our data provided further evidence that underscore current challenges in the reconciliation of molecular signatures vs clinical diagnoses. However, we cannot completely exclude the possibility that this can also be simply due to the fact that there were not enough samples to reveal all possible patterns. Although we performed 51 microarray (50 patients plus 1 pooled normal control) analyses for this study, using this particular cDNA chip, a relatively small number of patients were represented in each subgroup of uveitis (Table I).

Nevertheless, the data for the first time demonstrate a unique pattern of differential gene expression between autoimmune uveitis patients and normal donors, as well as possible molecular subtypes among autoimmune uveitis patients. To further explore the applications of gene expression profiling in autoimmune uveitis, we examined two other clinically relevant issues. The first question is whether there is a difference in gene expression pattern for the same patient at different clinical stages. Many uveitis patients will typically experience multiple episodes of occurrence during the course of their disease. However, it is not well defined whether those episodes were new or merely a continuation of the previous one. We examined the gene expression profiles of one particular patient with three defined clinical stages, active, quiescent, and recurrent/active over a span of >5 mo. We were surprised to see that the gene expression profiles from the three distinct stages are overall very similar (Fig. 6). This is a clear demonstration that the underlying mechanisms, represented by the consistent gene expression profile, have not been changed despite temporary clinical regression with therapy. We propose that this represents strong molecular evidence that clinical quiescence may not be a true reflection of underlying disease inactivity for autoimmune uveitis. Molecular analyses, such as gene profiling, may prove to be a more reliable and accurate method in predicting the clinical prognosis for recurrent diseases. We also examined gene expression profiles of a pair of male siblings who both have intermediate uveitis as a diagnosis. The gene expression profiles of the siblings were very similar to each other but dramatically different from the profile of normal controls (Fig. 7). Consistent with previous studies in both human and in a mouse uveitis model (22–24), our initial study on gene expression profile data from two male siblings who suffered from the same uveitis support the hypothesis that genetic factors are important in the pathogenesis of human autoimmune uveitis. However, more data will be needed to further validate this initial observation.

This study not only implicated IL-22 in human uveitis, but also the involvement of both IL-19, IL-20, and IL-25/IL-17E. It is of interest that IL-19 and IL-20, similar to IL-22, all belong to the IL-10 family. They share many biological characteristics with IL-22 and are shown to be associated with inflammatory disease (29). IL-25/IL-17E has been shown to boost type 2 immune response and allergy (42, 43). Although we do not currently understand the molecular mechanisms of the contribution of those cy-

tokines to autoimmune uveitis, our finding that all of those three genes are up-regulated in human autoimmune intraocular inflammatory disease may suggest a novel mechanism that contributes to human autoimmune intraocular inflammatory disease (uveitis). Consistent with a recent report that Th17 cells are involved in the pathogenesis of autoimmune uveitis (12), the finding that IL-22, IL-19, IL-20, and IL-25/IL-17E may contribute to the pathogenesis of autoimmune intraocular inflammatory disease sheds new insight on the molecular mechanisms of uveitis, as well as other autoimmune inflammatory diseases.

Acknowledgments

We thank NEI uveitis clinical fellows, clinical coordinators, and all patients who participated in this study.

Disclosures

The authors have no financial conflict of interest.

References

- Jabs, D. A., R. B. Nussenblatt, and J. T. Rosenbaum. 2005. Standardization of uveitis nomenclature for reporting clinical data: results of the First International Workshop. *Am. J. Ophthalmol.* 140: 509–516.
- Caspi, R. R. 1999. Immune mechanisms in uveitis. *Springer Semin. Immunopathol.* 21: 113–124.
- Nussenblatt, R. B. 1991. Proctor lecture: experimental autoimmune uveitis: mechanisms of disease and clinical therapeutic indications. *Invest. Ophthalmol. Vis. Sci.* 32: 3131–3141.
- Caspi, R. R. 2002. Th1 and Th2 responses in pathogenesis and regulation of experimental autoimmune uveoretinitis. *Int. Rev. Immunol.* 21: 197–208.
- Nussenblatt, R. B., and I. Scher. 1985. Effects of cyclosporine on T-cell subsets in experimental autoimmune uveitis. *Invest. Ophthalmol. Vis. Sci.* 26: 10–14.
- Rizzo, L. V., R. A. Morawetz, N. E. Miller-Rivero, R. Choi, B. Wiggert, C. C. Chan, H. C. Morse, 3rd, R. B. Nussenblatt, and R. R. Caspi. 1999. IL-4 and IL-10 are both required for the induction of oral tolerance. *J. Immunol.* 162: 2613–2622.
- Caspi, R. R., F. G. Roberge, C. C. Chan, B. Wiggert, G. J. Chader, L. A. Rozenszajn, Z. Lando, and R. B. Nussenblatt. 1988. A new model of autoimmune disease: experimental autoimmune uveoretinitis induced in mice with two different retinal antigens. *J. Immunol.* 140: 1490–1495.
- Ham, D. I., S. Gentleman, C. C. Chan, J. H. McDowell, T. M. Redmond, and I. Gery. 2002. RPE65 is highly uveitogenic in rats. *Invest. Ophthalmol. Vis. Sci.* 43: 2258–2263.
- Nussenblatt, R. B., T. Kuwabara, F. M. de Monasterio, and W. B. Wacker. 1981. S-antigen uveitis in primates: a new model for human disease. *Arch. Ophthalmol.* 99: 1090–1092.
- Nussenblatt, R. B., I. Gery, E. J. Ballantine, and W. B. Wacker. 1980. Cellular immune responsiveness of uveitis patients to retinal S-antigen. *Am. J. Ophthalmol.* 89: 173–179.
- de Smet, M. D., and C. C. Chan. 2001. Regulation of ocular inflammation: what experimental and human studies have taught us. *Prog. Retin. Eye Res.* 20: 761–797.
- Amadi-Obi, A., C. R. Yu, X. Liu, R. M. Mahdi, G. L. Clarke, R. B. Nussenblatt, I. Gery, Y. S. Lee, and C. E. Egwuagu. 2007. Th17 cells contribute to uveitis and scleritis and are expanded by IL-2 and inhibited by IL-27/STAT1. *Nat. Med.* 13: 711–718.
- Maminishkis, A., S. Chen, S. Jalickee, T. Banzon, G. Shi, F. E. Wang, T. Ehalt, J. A. Hammer, and S. S. Miller. 2006. Confluent monolayers of cultured human fetal retinal pigment epithelium exhibit morphology and physiology of native tissue. *Invest. Ophthalmol. Vis. Sci.* 47: 3612–3624.
- Li, Z., S. P. Mahesh, B. J. Kim, R. R. Buggage, and R. B. Nussenblatt. 2003. Expression of glucocorticoid induced TNF receptor family related protein (GITR) on peripheral T cells from normal human donors and patients with non-infectious uveitis. *J. Autoimmun.* 21: 83–92.
- Demir, T., A. Godekmerdan, M. Balbaba, P. Turkuoglu, F. Ilhan, and N. Demir. 2006. The effect of infliximab, cyclosporine A and recombinant IL-10 on vitreous cytokine levels in experimental autoimmune uveitis. *Indian J. Ophthalmol.* 54: 241–245.
- Hayashi, S., Y. Guex-Crosier, A. Delvaux, T. Velu, and F. G. Roberge. 1996. Interleukin 10 inhibits inflammatory cells infiltration in endotoxin-induced uveitis. *Graefes Arch. Clin. Exp. Ophthalmol.* 234: 633–636.
- Kreymborg, K., R. Etzensperger, L. Dumoutier, S. Haak, A. Rebollo, T. Buch, F. L. Heppner, J. C. Renauld, and B. Becher. 2007. IL-22 is expressed by Th17 cells in an IL-23-dependent fashion, but not required for the development of autoimmune encephalomyelitis. *J. Immunol.* 179: 8098–8104.
- Liang, S. C., X. Y. Tan, D. P. Luxenberg, R. Karim, K. Dunussi-Joannopoulos, M. Collins, and L. A. Fouser. 2006. Interleukin (IL)-22 and IL-17 are coexpressed by Th17 cells and cooperatively enhance expression of antimicrobial peptides. *J. Exp. Med.* 203: 2271–2279.

19. Sugimoto, K., A. Ogawa, E. Mizoguchi, Y. Shimomura, A. Andoh, A. K. Bhan, R. S. Blumberg, R. J. Xavier, and A. Mizoguchi. 2008. IL-22 ameliorates intestinal inflammation in a mouse model of ulcerative colitis. *J. Clin. Invest.* 118: 534–544.
20. Zheng, Y., D. M. Danilenko, P. Valdez, I. Kasman, J. Eastham-Anderson, J. Wu, and W. Ouyang. 2007. Interleukin-22, a T_H17 cytokine, mediates IL-23-induced dermal inflammation and acanthosis. *Nature* 445: 648–651.
21. Nussenblatt, R. B., and S. M. Whitcup. 2003. *Uveitis: Fundamentals and Clinical Practice*. Elsevier, New York.
22. Mochizuki, M., T. Kuwabara, C. C. Chan, R. B. Nussenblatt, D. D. Metcalfe, and I. Gery. 1984. An association between susceptibility to experimental autoimmune uveitis and choroidal mast cell numbers. *J. Immunol.* 133: 1699–1701.
23. Pennesi, G., and R. R. Caspi. 2002. Genetic control of susceptibility in clinical and experimental uveitis. *Int. Rev. Immunol.* 21: 67–88.
24. Sun, B., L. V. Rizzo, S. H. Sun, C. C. Chan, B. Wiggert, R. L. Wilder, and R. R. Caspi. 1997. Genetic susceptibility to experimental autoimmune uveitis involves more than a predisposition to generate a T helper-1-like or a T helper-2-like response. *J. Immunol.* 159: 1004–1011.
25. Staudt, L. M. 2003. Molecular diagnosis of the hematologic cancers. *N. Engl. J. Med.* 348: 1777–1785.
26. Harrington, L. E., R. D. Hatton, P. R. Mangan, H. Turner, T. L. Murphy, K. M. Murphy, and C. T. Weaver. 2005. Interleukin 17-producing $CD4^+$ effector T cells develop via a lineage distinct from the T helper type 1 and 2 lineages. *Nat. Immunol.* 6: 1123–1132.
27. Langrish, C. L., Y. Chen, W. M. Blumenschein, J. Mattson, B. Basham, J. D. Sedgwick, T. McClanahan, R. A. Kastelein, and D. J. Cua. 2005. IL-23 drives a pathogenic T cell population that induces autoimmune inflammation. *J. Exp. Med.* 201: 233–240.
28. Park, H., Z. Li, X. O. Yang, S. H. Chang, R. Nurieva, Y. H. Wang, Y. Wang, L. Hood, Z. Zhu, Q. Tian, and C. Dong. 2005. A distinct lineage of $CD4^+$ T cells regulates tissue inflammation by producing interleukin 17. *Nat. Immunol.* 6: 1133–1141.
29. Sabat, R., E. Wallace, S. Endesfelder, and K. Wolk. 2007. IL-19 and IL-20: two novel cytokines with importance in inflammatory diseases. *Expert Opin. Ther. Targets* 11: 601–612.
30. Kebir, H., K. Kreymborg, I. Ifergan, A. Dodelet-Devillers, R. Cayrol, M. Bernard, F. Giuliani, N. Arbour, B. Becher, and A. Prat. 2007. Human $TH17$ lymphocytes promote blood-brain barrier disruption and central nervous system inflammation. *Nat. Med.* 13: 1173–1175.
31. Ban, Y., and L. J. Rizzolo. 1997. A culture model of development reveals multiple properties of RPE tight junctions. *Mol. Vis.* 3: 18.
32. Bradfield, P. F., C. Scheiermann, S. Nourshargh, C. Ody, F. W. Lusinskas, G. E. Rainger, G. B. Nash, M. Miljkovic-Licina, M. Aurrand-Lions, and B. A. Imhof. 2007. JAM-C regulates unidirectional monocyte transendothelial migration in inflammation. *Blood* 110: 2545–2555.
33. Chang, C. W., L. Ye, D. M. Defoe, and R. B. Caldwell. 1997. Serum inhibits tight junction formation in cultured pigment epithelial cells. *Invest. Ophthalmol. Vis. Sci.* 38: 1082–1093.
34. Muller, W. A. 2003. Leukocyte-endothelial-cell interactions in leukocyte transmigration and the inflammatory response. *Trends Immunol.* 24: 327–334.
35. Zen, K., and C. A. Parkos. 2003. Leukocyte-epithelial interactions. *Curr. Opin. Cell Biol.* 15: 557–564.
36. Rosenwald, A., and L. M. Staudt. 2002. Clinical translation of gene expression profiling in lymphomas and leukemias. *Semin. Oncol.* 29: 258–263.
37. Villalta, D., R. Tozzoli, E. Tonutti, and N. Bizzaro. 2007. The laboratory approach to the diagnosis of autoimmune diseases: is it time to change? *Autoimmun. Rev.* 6: 359–365.
38. Whitney, L. W., S. K. Ludwin, H. F. McFarland, and W. E. Biddison. 2001. Microarray analysis of gene expression in multiple sclerosis and EAE identifies 5-lipoxygenase as a component of inflammatory lesions. *J. Neuroimmunol.* 121: 40–48.
39. Alizadeh, A. A., M. B. Eisen, R. E. Davis, C. Ma, I. S. Lossos, A. Rosenwald, J. C. Boldrick, H. Sabet, T. Tran, X. Yu, et al. 2000. Distinct types of diffuse large B-cell lymphoma identified by gene expression profiling. *Nature* 403: 503–511.
40. Rosenwald, A., G. Wright, W. C. Chan, J. M. Connors, E. Campo, R. I. Fisher, R. D. Gascoyne, H. K. Muller-Hermelink, E. B. Smeland, J. M. Giltman, et al. 2002. The use of molecular profiling to predict survival after chemotherapy for diffuse large-B-cell lymphoma. *N. Engl. J. Med.* 346: 1937–1947.
41. Shipp, M. A., K. N. Ross, P. Tamayo, A. P. Weng, J. L. Kutok, R. C. Aguiar, M. Gaasenbeek, M. Angelo, M. Reich, G. S. Pinkus, et al. 2002. Diffuse large B-cell lymphoma outcome prediction by gene-expression profiling and supervised machine learning. *Nat. Med.* 8: 68–74.
42. Wang, Y. H., P. Angkasekwinai, N. Lu, K. S. Voo, K. Arima, S. Hanabuchi, A. Hippe, C. J. Corrigan, C. Dong, B. Homey, et al. 2007. IL-25 augments type 2 immune responses by enhancing the expansion and functions of TSLP-DC-activated $Th2$ memory cells. *J. Exp. Med.* 204: 1837–1847.
43. Angkasekwinai, P., H. Park, Y. H. Wang, Y. H. Wang, S. H. Chang, D. B. Corry, Y. J. Liu, Z. Zhu, and C. Dong. 2007. Interleukin 25 promotes the initiation of proallergic type 2 responses. *J. Exp. Med.* 204: 1509–1517.